International Journal of Chemical, Materials and Biomolecular Sciences
ISSN: 2415-6620
Vol:5, No:11, 2011

Investigation of the Synthesis of Alcohols Byproducts in Fischer-Tropsch Synthesis on Modified Fe-Cu Catalyst: Reactivity and Mechanism

Wanyu Mao, Qiwen Sun, Weiyong Ying *, Dingye Fang

Abstract**—**The influence of copper promoters and reaction conditions on the formation of alcohols byproducts of a common Fischer-Tropsch synthesis used iron-based catalysts were investigated. A good compromise of 28%Cu/FeKLaSiO_2 can lead to the optimization of an improved Fischer-Tropsch catalyst. The product distribution shifts towards hydrocarbons with increasing the reaction temperature, while pressure promotes the formation of alcohols. It was found that the production of either alcohols or hydrocarbons followed A-S-F distributions, and their α parameters were essentially different which indicated a competition in the growing chain between the two species. TPD after acetaldehyde adsorption gave strong evidence of the insertion of a C_1 oxygen-containing species into an alkyl chain.

Keywords**—**Fischer-Tropsch synthesis, Fe-Cu catalyst, alcohols byproducts, reaction pathways

I. Introduction

THE Fischer-Tropsch synthesis (FTS) on iron catalysts is one of the most important routes for the production of liquid fuel from coal-derived syngas with low H_2/CO ratio. The product spectrum of Fischer-Tropsch synthesis with an iron catalyst consist of a complex multicomponent mixture of linear and branched hydrocarbons and oxygenates, especially at lower CO conversions. The oxygenated compounds have often been considered as unimportant by-products of the synthesis. However, synthesis pathways of higher alcohols and other oxygenates from syngas are relevant for a fundamental understanding of FTS. A substantial number of studies have been devoted to mechanism of formation of oxygenates while many questions remain unanswered.

Wanyu Mao is with Engineering Research Center of Large Scale Reactor Engineering and Technology, Ministry of Education, State Key Laboratory of Chemical Engineering, East China University of Science and Technology, Shanghai 200237 China (e-mail: cat.tou@163.com).

Qiwen Sun is with State Key Laboratory of Coal Liquefaction and Coal Chemical Technology, Shanghai 200237 China (e-mail: Sun_qiwen@ye-tech.com).

Weiyong Ying is with Engineering Research Center of Large Scale Reactor Engineering and Technology, Ministry of Education, State Key Laboratory of Chemical Engineering, East China University of Science and Technology, Shanghai 200237 China (corresponding author; phone: 86-21-64252193; fax: 86-21- 64252192; e-mail: wying@ecust.edu.cn).

Dingye Fang is with Engineering Research Center of Large Scale Reactor Engineering and Technology, Ministry of Education, State Key Laboratory of Chemical Engineering, East China University of Science and Technology, Shanghai 200237 China (e-mail: dyfang@ecust.edu.cn).

When then mechanism of the first carbon-carbon bond formation is concerned, a scheme based on the CO insertion into a CH_x-metal bond has been proposed on Rh [1] and Fe [2]. Others have suggested the reaction of CH_2 with formyl or methoxycarbonyl species on Rh [3] or proposed mechanism similar to the olefin hydroformylation (Mo) [4]. Katzer [5] noticed that methanol is formed through a non-dissociative way. Using labeled CO he conluded from the distribution of the labeled atoms in the reaction products that the methanol is not the precursor of the ethanol [6]. Studies with probe molecular, chemical trapping and coupling reactions have lead us to propose that the higher alcohol formation proceeds through coupling of a carbonic type hydrocarbonated species, which can contain several carbon atoms, with a C_1 oxygenated entity [7]. Recently, Tamaru [8] concluded to the intermediacy, of a surface acetate ion like structure. The same remark, concerning the rapid exchange CH_3CHO with H_2O can be formulated here. Tamaru, in accordance with the results of Somorjai [9], concluded that hydrocarbons and C_2 oxygenates have a common hydrocarbonated C_1 intermediate.

Mechanistic investigations indicated that surface hydrocarbon species appear, either as intermediates on the path to oxygenate formation, or as products of oxygenate decomposition. It is proposed that propagation of hydrocarbon chain involves stepwise addition of CH_x-monomeric units while the chain growth is terminated by CO insertion to form surface-bound acyl species. Hydrogenation of acyl may lead to oxygenates which can undergo secondary reactions [10].

The aim of the present work is to take into account the available data on the reaction mechanism to tempt to predict the overall alcohol selectivity and the percentage of chain growth on iron-copper based catalysts.

II. Experimental

A. Catalyst Preparation

Iron-based catalysts with or without promoter were prepared by conventional co-precipitation method. Typically, a mixture of iron and related metallic nitrates was introduced into a well-stirred thermo-stated vessel containing deionized water (0.1 l) at 343 ± 1 K. An aqueous solution of $NH_3 \cdot H_2O$ with concentration of 3 mol/L was added simultaneously into this precipitation vessel to maintain the pH at a constant value of 7.5 ± 0.2. After aging for 12 h, the precipitate was washed

thoroughly with deionized water, and was dried at 110℃ for 24 h and then calcined at 480℃ in air for 5 h. The obtained catalysts were composed of 100Fe/xCu/5K/5La/17SiO_2 in molar ratio. In addition, an unpromoted model catalyst with a composition of 100Fe/5K/5La/17SiO_2, an iron-free model catalyst with a composition of 100Cu/5K/5La/17SiO_2 were prepared to study the influence of modified component. The compositions of all samples were determined by ICP-AES emission spectrometry.

B. Reactivity Measurements

Apparatus

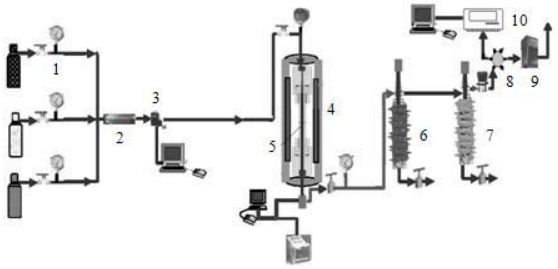

1-Stabilizing pressure valve; 2- Cleaning cartridge; 3- Mass flowmeter; 4-Heating oven; 5-Thermocouple; 6-Heat sink; 7-Cold trap; 8-Counterbalance valve; 9-Soup buble flowmeter; 10-GC
Fig. 1 Diagram for the catalyst evaluation unit

The catalytic performance testing was conducted with a fixed-bed, stainless flow micro-reactor (6 mm I.D.) containing 0.5 g of catalysts. The inlet gas flows were controled by a Brooks 5850E mass flow-mete. The formed liquid and wax products were condensed in a cold trap at 273 K and a warm trap at 423 K respectively. The tail gas was analyzed online by gas chromatography (model 7890A; Agilent) equipped with a 6-port sampling valve and two sampling loops. In one sampling loop, CO, CO_2, CH_4, N_2 and H_2 were analyzed with a molecular sieve 5A packed column (HP-PLOT, 30 m × 0.53 mm), a ProPack Q packed column (HP-PLOT, 30 m × 0.53 mm), and a thermal conductivity detector (TCD). In the other loop, C_1-C_6 hydrocarbons were analyzed with an Al_2O_3 capillary column (HP-AL/S, 30 m×0.530 mm) and a flame ionization detecter (FID). The products in oil and wax phase were analyzed off-line by GC (model 7890A; Agilent) with a phenyl polysiloxane capillary column (HP-5, 30 m×0.320 mm) and an FID. Oxygenates in water were analyzed off-line using GC (model 7890A; Agilent) with a PEG capillary column (DB-WAX, 30 m×0.320 mm) and an FID. A soup bubble flow meter was used to monitor the flow rate of tail gas.

Reduction conditions

For all experiments, the samples were reduced in a hydrogen flow at ambient pressure with a designed temperature-programmed procedure, which was employed as followed: RT→493 K with a rate of 1 K/min and keeping for 6 h. A steady gas flow of 1 $L \cdot h^{-1} \cdot g^{-1}_{cat}$ was maintained through the whole activation process.

Reaction conditions

After on-line activation described above, the temperature is decreased to above 473 K and the pressure is gradually increased to 4.0 MPa in H_2 atmosphere. Then syngas (H_2/CO =0.67) with 4 $L \cdot h^{-1} \cdot g^{-1}_{cat}$ was introduced into reactor, followed by a temperature-programmed procedure: 473 K→523 K in 3 h; 523 K→533 K in 1 h; 533 K→543 K in 1 h. The carbon balance was 100±5%. The yields, conversions and selectivities were determined with an accuracy of 5%.

ICP-AES emission spectrometry:

0.0200 g of the samples were dissolved in Hydrofluoric acid and Aqua regia in turn and heated to wet dry (353 K). Then they were metered to 100 ml Clarified solution. The tests were performed with Varian 710ES emission spectrometry.

Power X-ray diffraction (XRD):

Power X-ray diffraction patterns of the catalysts were recorded on a Bruker D8 advanced diffractometer using Cu Kα radiation (λ=1.54056 A) at 40 kV and 100mA.

Temperature programmed reduction of H_2:

The tests were performed with Autochem II 2920 model multifunctional adsorption instrument (Micromeritics Comoany, USA). H_2 consumption was monitored with a thermal conductivity detector (TCD). An in-line liquid-nitrogen trap located between the reactor and the TCD was used to continuously remove water produced during reduction. Typically, the samples (0.5 g) were flushed at 773 K in a helium flow of 50 ml/min for 30 min, and then cooled to 323 K. After stabilization, the temperature was raised with a slope of 10 K/min up to 1173 K under a 30 ml/min 10% H_2 in Ar mixture.

Temperature programmed desorption of acetaldehyde

They were performed in equipment the same to that used in the TPR tests. After reducing the catalyst with the same procedure as in the catalytic tests, the catalyst was cooled to 308 K in a 4 $L \cdot h^{-1} \cdot g^{-1}_{cat}$ He. CH_3CHO was chemisorbed by passing a 4 $L \cdot h^{-1} \cdot g^{-1}_{cat}$ 1.01% CH_3CHO in He mixture for 30 min. After flushing again with 4 $L \cdot h^{-1} \cdot g^{-1}_{cat}$ He for 2 hours, the temperature was increased with a 5 K/min slope up to 773 K. Desorption products were analyzed and identified by on-line gas chromatograph fed by heating multi-position sampling valves. Acetaldehyde, acetone, ethanol were detected after separation on HP-PLOT-Q (FID), carbon monoxide and dioxide on INNO Wax (TCD). Hydrogen, water were not analyzed.

III. Results And Discussion

A. Reducibility of the catalysts

H_2-TPR was used to investigate the effect of Cu on the reduction behavior. Fig. 2 shows H_2-TPR profiles of the five catalysts with different compositions. The H_2-TPR profiles of the copper-modified iron catalysts are generally similar with each other. TPR experiments show that copper favors the reduction of iron. The spectra given in Fig. 2 shows that under our conditions the reduction peak maximums for the systems are situated at 473K and around and the high-temperature TPR profile shows a broad peak.

The amount of H_2 consumed during different reduction stages, obtained from integrating the area of the corresponding reduction peak, is summarized in Table I. For the $FeCuKLa/SiO_2$ catalyst, the amounts of H_2 consumption for reduction peaks at lower temperature range (< 800 K) (Table 1) are close to the theoretical value for the reduction of metal oxides to Cu, LaO and Fe_3O_4 (0.24, 0.31, 0.35, 0.37, 0.44 mol H_2 / mol M with the increase of x). The peaks at higher temperature (above 800 K) correspond to the reduction of Fe_3O_4 to Fe, and the H_2 consumptions are consistent with theoretical values (1.33 mol H_2 / mol Fe). Two peaks of H_2 consumption were observed at 516 and 555 K for the iron-free catalyst (see Fig. 3), corresponding to the reduction of highly dispersed CuO, La_2O_3 and the reduction of bulk CuO, La_2O_3 [11], [12]. The H_2 consumptions were very close to the theoretical value (0.98 mol H_2 / mol M), which indicated complete reduction.

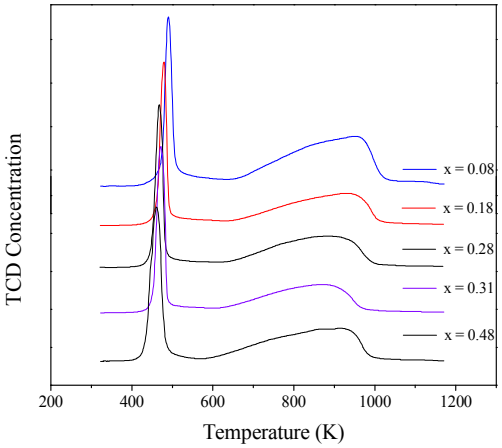

Fig. 2 Temperature-programmed reduction (TPR) spectra

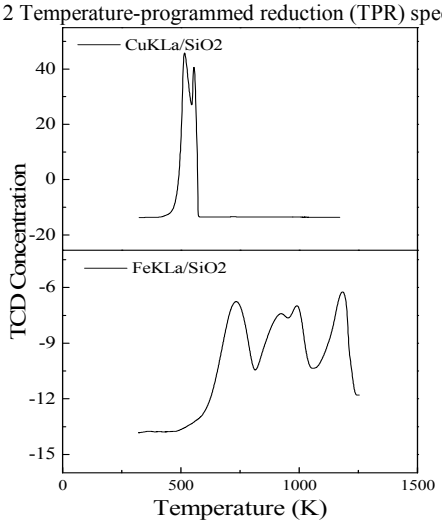

Fig. 3 H_2-TPR profiles for $CuKLa/SiO_2$ and $FeKLa/SiO_2$ catalyst

In the condition of $FeKLa/SiO_2$ catalyst, the H_2 consumption of the peak at 733 K (0.33 mol H_2 / mol M) and 921 K is close to the theoretical value for the reduction of α-Fe_2O_3 to FeO. It is clearly shown that the phase transformations of the iron based catalysts during TPR process are $Fe_2O_3 \rightarrow Fe_3O_4 \rightarrow FeO \rightarrow Fe$. There should be three reduction peaks corresponding to $Fe_2O_3 \rightarrow Fe_3O_4$, $Fe_3O_4 \rightarrow FeO$ and $FeO \rightarrow Fe$ process respectively. Our spectra shows a broad peak for the $Fe_3O_4 \rightarrow FeO$ and $FeO \rightarrow Fe$ process. According to Munteanu et. al [13] who calculated kinetic parameters of reduction process of Fe_2O_3, the activation energy and rate constants for $Fe_3O_4 \rightarrow FeO$ and $FeO \rightarrow Fe$ are similar, which indicated that Fe_3O_4 reduced to Fe directly. Thus the TPR profile shows a broad peak for $Fe_3O_4 \rightarrow FeO \rightarrow Fe$. Fig. 4 shows the fitted superposition of two hydrogen consumption peaks at around 900 K for the $FeCuKLa/SiO_2$ catalyst (x=0.08).

TABLE I
QUANTITATIVE RESULTS OF H_2 CONSUMPTION FOR CATALYSTS IN H_2-TPR[a]

Catalysts	Peak (K)	H_2 consumption	
		mol H_2 / mol M[b]	mol H_2 / mol Fe
$CuKLa/SiO_2$	516	0.70	
	555	0.24	
$FeCuKLa/SiO_2$(x=0.08)	490	0.22	
	950		1.03
$FeCuKLa/SiO_2$(x=0.18)	480	0.30	
	931		1.17
$FeCuKLa/SiO_2$(x=0.28)	470	0.32	
	888		1.25
$FeCuKLa/SiO_2$(x=0.31)	469	0.35	
	870		1.25
$FeCuKLa/SiO_2$(x=0.48)	461	0.38	
	914		1.31
$FeKLa/SiO_2$	733	0.33	
	921	0.15	
	990		0.21
	1182		0.26

[a] The H_2 consumption was measured from the area under the corresponding peak.
[b] M = Fe + Cu + La.

B. Comparison with monometallic systems

Table II shows the catalytic behavior of monometallic and bimetallic catalysts. From the table we can see that Fe-Cu catalyst showed the reaction behavior of F-T synthesis rather than mixed alcohols synthesis stemmed from the strong activation tendency of iron towards CO in dissociative mode. Under our reaction conditions, methanol is the main product on $CuKLa/SiO_2$, whereas on the $FeCuKLa/SiO_2$ catalyst higher alcohols as well as hydrocarbons are formed. The production of C_2^+ alcohols in the alcohol fraction amounts to 79%.

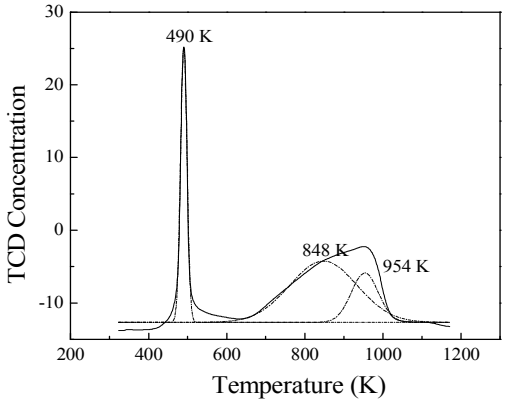

Fig. 4 Lorentzian multi-peak fitting curves for $FeCuKLa/SiO_2$ catalyst (x=0.08)

$FeKLa/SiO_2$ also gives hydrocarbons and alcohols, the higher alcohol fraction represents 78% of the total alcohol production. However the Fe-Cu has an activity which is almost five times as high as that of the monometallic catalysts with a higher total alcohol selectivity.

TABLE II
CATALYTIC BEHAVIOR OF MONOMETALLIC AND BIMETALLIC CATALYSTS

Catalysts	Convertion (%)	Selectivities(wt.%)			C_2^+OH/ROH (wt.%)
		MeOH	C_2^+OH	HC	
$CuKLa/SiO_2$	5.92	53.39	3.06	43.55	5.42
$FeCuKLa/SiO_2$ (x=0.08)	21.09	2.31	8.78	88.91	79.15
$FeKLa/SiO_2$	4.32	2.86	10.24	86.90	78.16

Reaction conditions: H_2/CO=0.67, 4 $L \cdot h^{-1} \cdot g^{-1}_{cat}$, P=4 MPa, T=543 K.

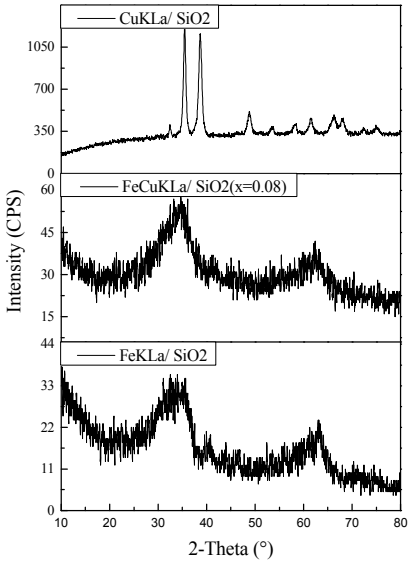

Fig. 5 XRD patterns of fresh catalyst samples

The XRD patterns of the fresh catalysts are shown in figure 5. For the three samples, the diffraction peaks ascribed to K, La species are too weak to be identified. From the figure we can see that the XRD patterns of three catalysts are obviously different. Two broad diffraction peaks around 2θ values of 34° and 64° appear in the patterns of catalyst $FeKLa/SiO_2$ and $FeCuKLa/SiO_2$(x=0.08). This result corresponds to C.H.Zhang, et al. [14], who reported that the incorporation of SiO_2 decrease the crystallite size of iron oxides. The broad peaks are characteristic of small particles with crystallite diameter lower than 15 nm [15]. The diffractogram has a maximum relative intensity at 2θ of 34.7° and 32.6°, which coincides with the maximum characteristic peak of maghemite (γ-Fe_2O_3) and maybe indicative of the existence of γ-Fe_2O_3 in the two catalysts. The typical diffraction peaks of CuO at 2θ of 38.7° and 48.9° and Cu_2O at 2θ of 35.5° appear in the patterns of catalyst $CuKLa/SiO_2$.

C. Influence of the copper content

Five catalysts with different Cu contents were prepared and tested in CO + H_2 reactions and the results are compared in Table III and IV. It can be seen that the addition of only a slight amount of copper changed evidently the performance for CO hydrogenation, in which a drastic decrease in the CH_4 selectivity and a simultaneous increase of C_2^+OH and C_2^+HC yields. This have also been reported for cobalt-containing catalysts by Takeuchi et al. [16]. A common intermediate for the formation of both compounds was proposed. A competition in the growing chain between CH_2 addtion leading to hydrocarbons and an insertion of a C_1 oxygenated species (formyl or adsorbed CO) resulting in alcohol formation could be observed.

A good 94.72% content of C_2^+ hydrocarbons in the hydrocarbon mixture and a high hydrocarbon selectivity is observed with a 28% copper loading.

Thus the amount of copper influences the formation both to hydrocarbons and alcohols and only a good compromise can lead to the optimization of an improved Fischer-Tropsch catalyst.

D.Alcohol distribution

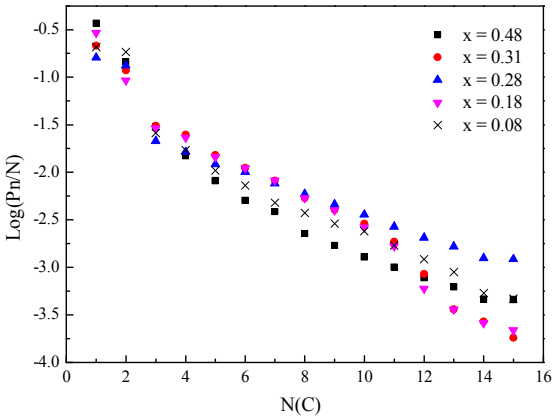

Fig. 6 Schulz-Flory plot of alcohol formation on promoted catalysts. Reaction conditions: H_2/CO=0.67, 4 $L \cdot h^{-1} \cdot g^{-1}_{cat}$, P=4 MPa, T=543 K.

The oxygen-containing products of FTS have received much more attention since the pioneering work of Emmett and coworkers [17]. Though the content of the oxygenates is small relative to the total products, it has significant influence on the upgrading of primary FTS products. Therefore, discussing the selectivity to oxygenates in total products is important. It may also provide some valuable information for understanding the complex FTS reaction mechanism from the point of view of conservation of mass.

The acids and alcohols with lower molecular weight are mainly dissolved in water, while alcohols with higher molecular weight are mainly dissolved in oil. The product distributions are listed in Table Ⅳ. The alcohols obtained on the $FeCuKLa/SiO_2$ catalysts were mainly linear, and less than 20% iso-alcohols were observed in the C_4 alcohol fraction. In all cases, a little amount of other oxygenates, less than 3 wt.% in liquid products, including aldehydes, ketones, esters and ethers were also detected. The hydrocarbons were mainly composed of C_2-C_5 and C_6-C_{12} olefins and the CH_4 selectivity was relatively lower compared with monometallic catalysts.The

TABLE III
CATALYTIC PERFORMANCE[a]

Catalysts	Con(%)	Yield (g/kg$_{catal}$/h)	Yield (g/kg$_{catal}$/h)	Selectivity (wt.%) (CO_2 excluded)			α parameters[b]	
		ROH	HC	S_{ROH}	S_{CH4}	S_{HC}	ROH	HC
FeKLa/SiO_2	4.32	3.51	23.27	13.10	17.35	69.55	0.28	0.58
FeCuKLa/SiO_2(x=0.08)	21.09	16.35	131.09	11.09	4.95	83.96	0.71	0.81
FeCuKLa/SiO_2(x=0.18)	21.06	13.23	110.92	10.66	5.83	83.51	0.65	0.80
FeCuKLa/SiO_2(x=0.28)	17.29	10.93	130.49	7.73	4.88	87.39	0.78	0.86
FeCuKLa/SiO_2(x=0.31)	21.14	14.13	126.02	10.08	5.87	84.05	0.65	0.79
FeCuKLa/SiO_2(x=0.48)	13.81	9.26	73.46	11.20	10.71	78.09	0.71	0.77
CuKLa/SiO_2	5.92	14.00	10.80	56.45	10.40	33.15	0.48	0.63

[a] Reaction conditions: H_2/CO=0.67, 4 $L \cdot h^{-1} \cdot g^{-1}_{cat}$, P=4 MPa, T=543 K.
[b] Less than 15C

TABLE IV
PRODUCT DISTRIBUTIONS OF MODEL CATALYSTS

Catalysts	ROH(wt.%)							HC(wt.%)					
	C_1	C_2	C_3	C_4	C_5	C_6	C_7^+	C_1	C_{2-5}	C_{6-12}	C_{13-20}	C_{21-26}	C_{27}^+
FeKLa/SiO_2	21.84	70.61	4.80	1.87	0.67	0.21	0.00	19.96	56.10	23.94	0.00	0.00	0.00
FeCuKLa/SiO_2(x=0.08)	20.85	36.88	7.78	6.83	5.21	4.37	18.09	5.56	20.67	38.10	22.04	9.12	4.46
FeCuKLa/SiO_2(x=0.18)	29.37	18.49	8.69	9.25	7.22	6.63	20.36	6.53	29.34	41.32	15.84	4.54	2.43
FeCuKLa/SiO_2(x=0.28)	16.05	26.53	6.41	6.57	6.05	6.02	32.36	5.28	18.94	25.81	28.35	14.46	7.17
FeCuKLa/SiO_2(x=0.31)	21.51	23.57	9.23	9.94	7.59	6.68	21.47	6.53	32.22	33.57	15.38	7.15	5.16
FeCuKLa/SiO_2(x=0.48)	36.80	29.08	8.99	5.99	4.09	3.04	12.02	12.06	36.95	19.18	18.41	8.86	5.55
CuKLa/SiO_2	94.58	2.50	1.13	0.92	0.39	0.25	0.24	23.87	51.40	24.72	0.00	0.00	0.00

Reaction conditions: H_2/CO=0.67, 4 $L \cdot h^{-1} \cdot g^{-1}_{cat}$, P=4 MPa, T=543 K.

carbon number distributions (less than 15C) of alcohols over this FeCuK/SiO_2 catalyst followed excellently Anderson-Schulz-Flory (ASF) plots (logarithm of mole fraction vs. carbon number) (see Fig. 6). A slight difference appears for ethanol formation which is higher than expected. Carbon number distributions of C_{15}^+ alcohols deviate from the ASF plots. Some researchers proposed that, alcohols' re-adsorption on the active sites and further participation in the chain growth caused the deviation [18].

E. Influence of the reaction temperature and pressure

The reactivity results at different temperatures and pressures are listed in Table V for the FeCuKLa/SiO_2(x=0.08) catalyst. Figure 7 represents the reactivity as a function of temperature and pressure. It is shown that with increasing temperature from 523 to 553 K (3.75 MPa), the CO convertion increased from 12.83% to 24.65%. It seems that increasing temperature makes the selectivities for alcohols decrease from 13.76% to 8.69%, while hydrocarbons increase from 86.24% to 91.31%. The methane selectivity increase with increasing temperature. Y. Liu thought it is owing to the increased H_2/CO ratio inside the reactor [19].

In commercial process, the FTS reaction usually operates under high pressure. The effect of reaction pressure on the catalytic performance, shown in Table V, shows that the CO convertion increased with the increasing pressure from 3.00 to 3.75 MPa. This is due to the enhanced concentration of active surface carbon species with increasing pressure and the improved collision probability of the catalysts and reactants. It is clear that pressure promotes the formation of alcohols. However, yields of both alcohols and hydrocarbons increased which may due to the favor of the conversion of CO. The results of the detailed analysis of the hydrocarbons and alcohols produced have been interpreted in terms of the Schulz-Flory distributions, as illustrated in Table VI. As we mentioned above, carbon number distributions of C_{15}^+ alcohols deviate from the ASF plots. It is generally assumed, that the olefin readsorption probability increases with increasing carbon number due to increased residence times of longer chains in the liquid-filled pores of the catalyst [20]. For that reason, only the $C_1 - C_{15}$ fraction has been taken into account. A linear distribution, in agreement with the Schulz–Flory equation, is observed. However, as is usual [21], the values for the C_1 and C_2 products are situated above and below the line respectively. The change trends of chain growth probability (α parameter) for alcohols and hydrocarbons with reaction temperature and

TABLE V
INFLUENCE OF THE REACTION TEMPERATURE AND PRESSURE ON THE REACTIVITY OF A FECUKLA/SIO2(X=0.08) CATALYST[a]

T(℃)	P(Mpa)	Con(%)	Yield ($g/kg_{catal}/h$) ROH	Yield ($g/kg_{catal}/h$) HC	Selectivity (wt.%) (CO_2 excluded) S_{ROH}(wt%)	S_{CH4}	S_{HC}	α parameters ROH	HC
523 K	3.00MPa	7.95	8.69	29.66	12.27	7.61	80.12	0.68	0.78
	3.25MPa	10.70	11.67	39.82	12.55	6.23	81.22	0.66	0.78
	3.50MPa	12.64	12.80	44.58	13.03	6.05	80.92	0.69	0.78
	3.75MPa	12.83	14.91	54.55	13.76	5.83	80.41	0.70	0.78
533 K	3.00MPa	12.65	10.55	50.02	10.78	5.81	83.40	0.69	0.79
	3.25MPa	15.15	12.58	55.55	10.89	6.82	82.29	0.69	0.77
	3.50MPa	15.39	14.03	62.38	11.03	6.10	82.87	0.70	0.78
	3.75MPa	16.38	17.04	88.60	11.30	5.09	83.62	0.72	0.80
543 K	3.00MPa	17.49	11.83	59.26	9.23	7.77	83.00	0.67	0.76
	3.25MPa	17.94	12.72	60.39	9.58	7.60	82.82	0.66	0.75
	3.50MPa	19.13	13.91	63.73	9.86	7.73	82.42	0.66	0.75
	3.75MPa	20.33	14.86	85.66	10.20	5.01	84.79	0.73	0.81
553 K	3.00MPa	22.94	12.65	66.22	7.99	9.31	82.70	0.65	0.74
	3.25MPa	23.18	12.45	63.76	8.29	9.27	82.43	0.65	0.75
	3.50MPa	23.60	13.54	66.95	8.61	9.19	82.20	0.65	0.75
	3.75MPa	24.65	14.28	73.34	8.69	8.84	82.46	0.65	0.74

[a] Reaction conditions: $H_2/CO=0.67$, 4 $L{\cdot}h^{-1}{\cdot}g^{-1}_{cat}$,.

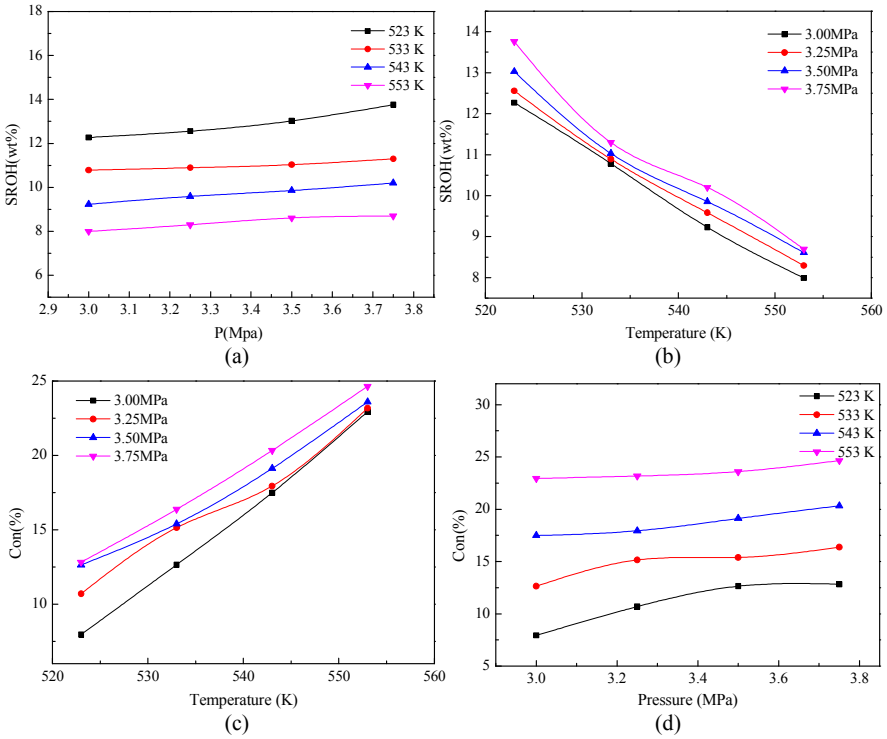

Fig. 7 The influence of reaction condition（temperature、pressure） on CO conversion of a FeCuKLa/SiO2(x=0.08) catalyst. Reaction conditions: $H_2/CO=0.67$, 4 $L{\cdot}h^{-1}{\cdot}g^{-1}_{cat}$,.

pressure, calculated on the basis of ASF distribution function, are presented in Figure 8 and 9. The corresponding graphs for the alcohols differ somewhat from those of the corresponding hydrocarbons. Unlike Co-Cu catalysts reported in the literature,

TABLE VI
SELECTIVITY FOR HYDROCARBONS AND ALCOHOLS ON A FECUKLA/ SIO2(X=0.08) CATALYST AT DIFFERENT TEMPERATURES AND PRESSURES.[a]

T(℃)	P(Mpa)	ROH(wt.%)							HC(wt.%)					
		C_1	C_2	C_3	C_4	C_5	C_6	C_7^+	C_1	C_{2-5}	C_{6-12}	C_{13-20}	C_{21-26}	C_{27}^+
523 K	3.00MPa	17.46	41.87	7.12	6.63	5.65	4.59	16.68	8.67	36.28	31.80	15.22	3.31	1.60
	3.25MPa	22.13	21.30	9.67	9.71	8.80	6.78	21.62	7.13	30.91	40.70	13.25	4.81	3.21
	3.50MPa	23.08	21.21	9.99	9.80	8.88	7.01	20.03	11.88	49.41	10.09	7.82	9.72	11.08
	3.75MPa	24.87	20.12	10.22	9.27	7.79	5.93	21.80	6.76	28.35	29.95	16.32	8.39	10.22
533 K	3.00MPa	18.40	17.08	11.37	10.80	9.78	7.35	25.22	6.51	28.81	40.76	15.58	4.33	4.01
	3.25MPa	19.68	18.23	11.32	10.50	9.30	6.97	24.00	7.65	33.38	34.75	14.76	4.89	4.56
	3.50MPa	19.53	18.03	11.36	10.50	9.13	6.78	24.66	6.85	30.11	35.84	14.71	5.92	6.57
	3.75MPa	16.35	14.87	10.05	10.62	9.94	7.73	30.44	5.73	24.91	33.05	18.10	8.36	9.84
543 K	3.00MPa	20.14	19.09	11.96	10.44	9.46	6.75	22.15	8.57	36.49	35.60	12.96	3.24	3.14
	3.25MPa	19.48	18.42	12.91	11.24	9.80	6.86	21.29	8.40	36.82	36.96	12.05	3.00	2.77
	3.50MPa	18.73	18.19	12.98	11.31	9.82	6.92	22.04	8.57	36.81	36.51	11.67	3.32	3.12
	3.75MPa	19.12	33.63	7.44	7.09	5.66	4.89	22.16	5.58	20.68	38.17	22.09	9.01	4.47
553 K	3.00MPa	21.50	20.30	13.45	10.62	9.16	6.10	18.87	10.12	39.58	35.26	10.37	2.43	2.23
	3.25MPa	20.82	19.45	12.80	10.74	9.57	6.45	20.17	10.11	39.43	34.72	10.95	2.53	2.26
	3.50MPa	20.37	19.19	13.02	10.94	9.73	6.88	19.87	10.05	39.86	35.53	10.50	2.16	1.91
	3.75MPa	19.01	18.62	13.35	11.37	10.00	7.00	20.64	9.69	39.01	35.27	10.70	2.81	2.52

[a] Reaction conditions: $H_2/CO=0.67$, 4 $L \cdot h^{-1} \cdot g^{-1}_{cat}$.

over which the α parameters, for both alcohols and hydrocarbons appeared in parallel [7], the Fe-Cu based catalyst showed different α parameters for two products. This discrepancy should be due to the bulk compositions of the two catalyst systems. Unequal α parameters between hydrocarbons and alcohols indicated a competition in the growing chain between the two species. As for hydrocarbon products, it was noted that the α parameter generally shows a monotonous decrease with the increasing reaction temperature. While this tendency cannot be observed in the alcohol products.

F. Relation between catalytic behavior and characterization - TPD of acetaldehyde

The study of the behavior of the acyl can give useful indications on the alcohols formation routes. The organic compound which is nearest to an acyl is the adsorbed aldehyde. Therefore, the TPD of acetaldehyde is used to predict the alcohol chain-growth probability by relating it to the amount of desorbed acetone produced by the surface trapping of an acetyl surface species by CH_3. On $FeCuKLa/SiO_2$ catalysts, acetone is the major obtained product and the peak which seems to be the most important at low temperature is that of acetone. These results are in good agreement with the previous data given by Kiennemann [22].

According to Kiennemann et al. three areas of desorption products can be observed:

353-393K CH_3CHO and C_2H_5OH,

At about 473K acetone and butyraldehyde,

573-673K acetone, C_3 hydrocarbons, methane, C_4 hydrocarbons and carbon dioxide.

According to the literature [4], higher alcohols are produced through the insertion of an oxygenated C_1 entity into a CH_x or hydrocarbonated species. That means surface species would be formed (). The proposed route is:

$+ \quad -CH_3 \rightarrow (CH_3)_2C=O \rightarrow (CH_3)_2COH.$

This means the amount of acetone correlates with the formation of acyl species. The products obtained in the TPD can be considered as representing the three pathways of acetaldehyde: hydrogenation, oxidation and acyl species formation. If the route proposed existed, the last pathway is characterized by the acetone formation. Thus for a given catalyst, the higher the amount of acetone formed, the more the last pathway is favored. Since the distribution of the alcohols followed the ASF plots, if the trend to insert CO for the C_2 oxygenates formation is proved it can also be considered for the C_3^+ oxygenates.

Comparing the data in Fig. 10, the acetone desorption at 473 K and around for the catalysts prepared in the present study, it can be observed that on Fe-Cu catalysts, the selectivity of alcohols can roughly be related to the amount of desorbed acetone (e.g. 11.09 and 10.66 wt.% of alcohols corresponds to 10.80 and 8.56 A.U. of acetone respectively). That means the

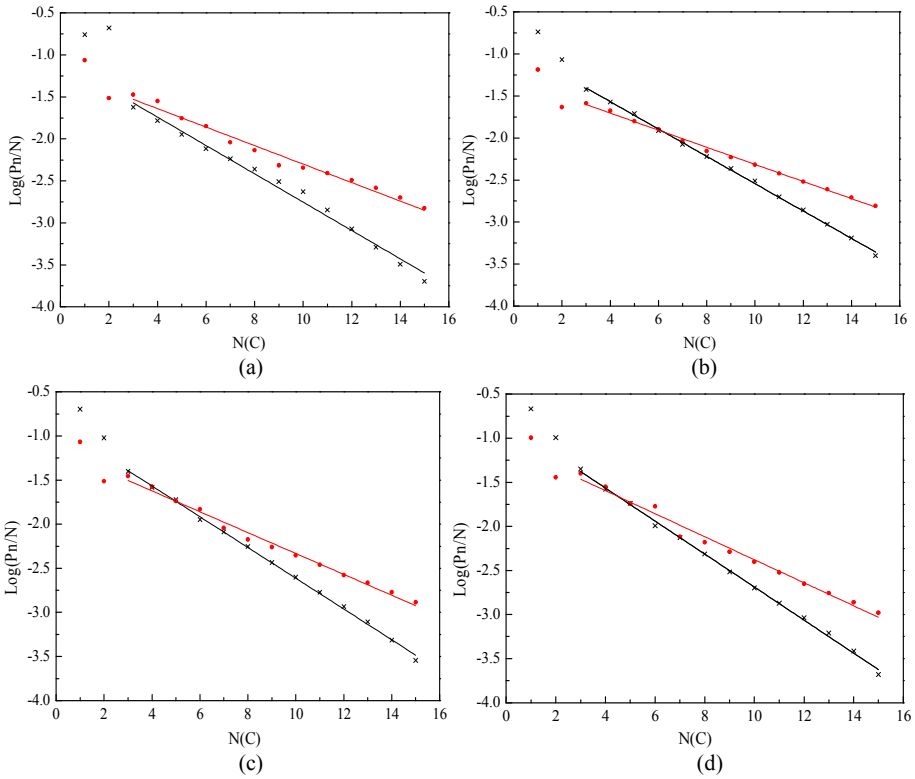

Fig. 8 The ASF distribution of product on the FeCuKLa/ SiO_2 catalyst (x=0.08), ×-alcohol,●-hydrocarbon
a – 3.00 MPa, 523 K; b – 3.00 MPa, 533 K; c – 3.00 MPa, 543 K; d – 3.00 MPa, 553 K

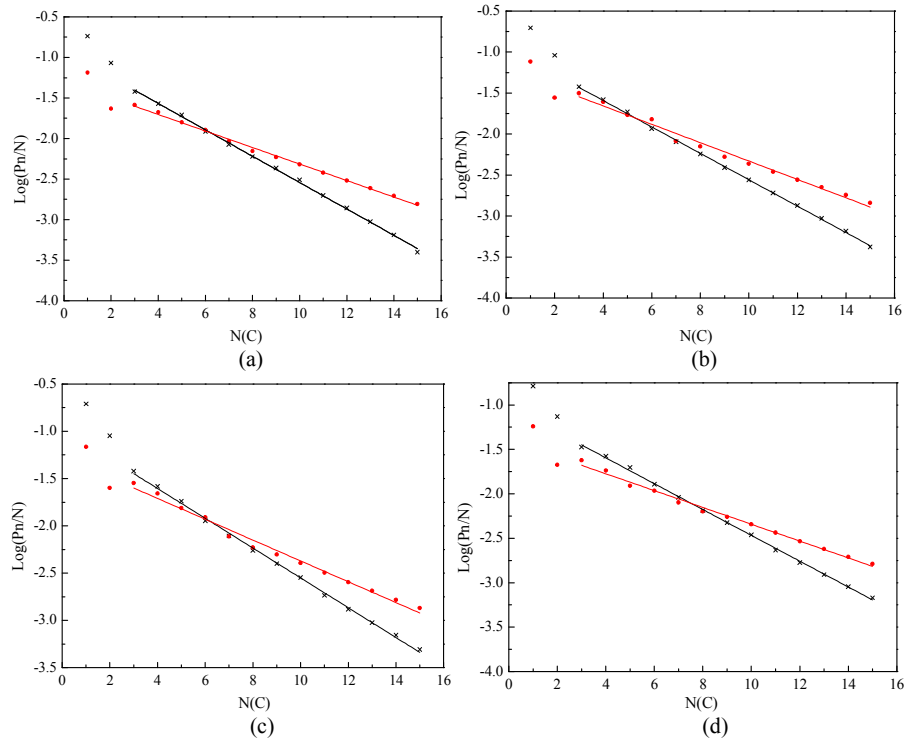

Fig. 9 The ASF distribution of product on the FeCuKLa/ SiO_2 catalyst (x=0.08), ×-alcohol,●-hydrocarbon
a – 3.00 MPa, 533 K; b – 3.25 MPa, 533 K; c – 3.50 MPa, 533 K; d – 3.75 MPa, 533 K

percentage of the peak area of low-temperature acetone could be well correlate with the ability to produce alcohols of the catalyst.

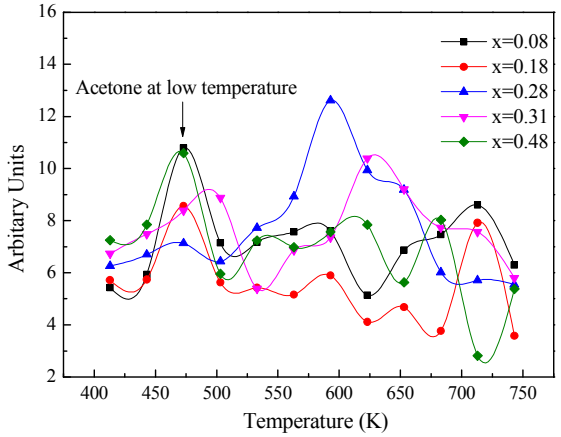

Fig. 10 TPD spectra of CH_3COCH_3 after CH_3CHO loadingReaction conditions: H_2/CO=0.67, 4 $L \cdot h^{-1} \cdot g^{-1}_{cat}$, P=4 MPa, T=543 K.

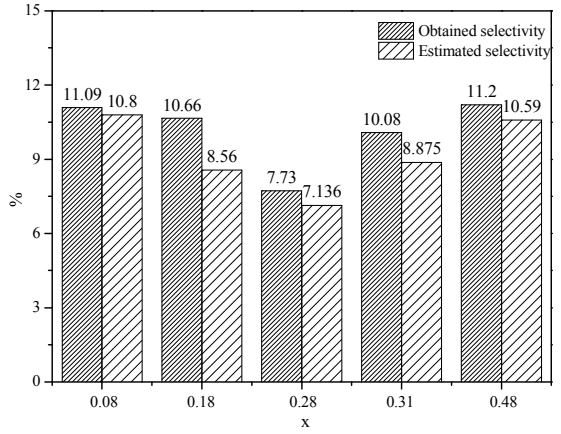

Fig. 11 Comparison of the computed and measured alcohol chain growth probability. Reaction conditions: H_2/CO=0.67, 4 $L \cdot h^{-1} \cdot g^{-1}_{cat}$, P=4 MPa, T=543 K

IV. Conclusion

A common FTS used iron-base catalyst was prepared. The influence of copper promoter and reaction conditions on the reactivities were investigated and compared. The amount of copper influences the formation both to hydrocarbons and alcohols and only a good compromise can lead to the optimization of an improved Fischer-Tropsch catalyst. The product distribution shifts towards hydrocarbons with increasing the reaction temperature, while pressure promotes the formation of alcohols.

In the present work, it has been shown that the alcohols productivities of Fe-Cu catalysts are different from that of cobalt containing catalysts. The alcohol chain growth follows an ASF distribution with extremely different chain growth probabilities with the hydrocarbon chain growth. The distributions of the alcohols compared to those of the hydrocarbons indicate that they have a competition in the growing chain between the two species. The alcohol distributions as well as the results of TPD after acetaldehyde adsorption are in good agreement with a mechanism of insertion of a C_1-oxygen containing species into an alkyl growing chain.

Acknowledgment

The authors gratefully acknowledge the financial support of the Coal Convertion Progress Chemistry and Engineering basic research Program of China (Grant No. 2010CB736203) and Shanghai Yankuang Energy R&D Co., Ltd.

References

[1] M. Ichikawa, T. Fukushima, "Mechanism of syngas conversion into C_2-oxygenates such as ethanol catalysed on a SiO_2-supported Rh-Ti catalyst", J. Chem. Soc. Chem. Comm., vol. 1985, pp. 321-323, 1985.
[2] M. Pijolat, V. Perrichon, "Synthesis of alcohols from CO and H_2 on a $Fe/A1_2O_3$ catalyst at 8-30 bars pressure", Appl. Catal., vol. 13, pp. 321-333, Jan. 1985.
[3] J. Hackenbruch, W. Keim, M. Roper, H. Strutz, "Mechanistic considerations for the formation of oxygenated species in the Fischer-Tropsch synthesis", J. Mol. Cat., vol. 26, pp. 129-134, Feb. 1985.
[4] T. Tatsumi, A. Muramatsu, K Yokota, H. Tominaga, "Mechanistic study on the alcohol synthesis over molybdenum catalysts: Addition of probe molecules to CO-H_2", J. Catal., vol. 115, pp. 388-398, Feb. 1989.
[5] A. Takeuchi, J.R. Katzer, "Mechanism of methanol formation", J. Phys. Chem., vol. 85, pp. 937-939, Apr. 1981.
[6] A. Takeuchi, J.R. Katzer, "Ethanol formation mechanism from carbon monoxide + molecular hydrogen", J. Phys. Chem., vol. 86, pp. 2438-2441, June 1982.
[7] A. Kiennemann, C. Diagne, J.P. Hindermann P. Chaumette, Ph. Courty, "Higher alcohols synthesis from CO+2H_2 on cobalt-copper catalyst: Use of probe molecules and chemical trapping in the study of the reaction mechanism", Appl. Catal., vol. 53, pp. 197-216, Sep. 1989.
[8] H. Orita, S. Naito, K. Tamaru, "Mechanism of acetaldehye formation from the carbon monoxide-hydrogen reaction below atmospheric pressure over supported Rh catalysts", J. Chem. Soc. Chem. Comm., vol. 1984, pp. 150-151, 1984.
[9] D.G. Castner, R.L. Blackadar, G.A. Somorjai, "CO hydrogenation over clean and oxidized rhodium foil and single crystal catalysts. Correlations of catalyst activity, selectivity, and surface composition", J. Catal., vol. 66, pp. 257-266, Dec. 1980.
[10] P. Biloen, M.W.H. Sachtler, "Mechanism of hydrocarbon synthesis over Fischer-Tropsch catalysts", Adv. Catal., vol. 30, pp. 165-216, 1981.
[11] M. Shimokawabe, H. Asakawa, N. Takezawa, "Characterization of copper/zirconia catalysts prepared by an impregnation method", Appl. Catal., vol. 59, pp. 45-58, Mar. 1990.
[12] R. Zhou, T. Yu, X. Jiang, F Chen, X. Zheng, "Temperature-programmed reduction and temperature-programmed desorption studies of CuO/ZrO_2 catalysts", Appl. Surf. Sci., vol. 148, pp. 263-270, July 1990.
[13] G. Munteanu, L. Ilieva, D. Andreeva, "Kinetic parameters obtained from TPR data for α-Fe_2O_3 and Au/α-Fe_2O_3 systems", Thermochimica Acta, vol. 291, pp. 171-177, Apr. 1997.
[14] C.H. Zhang, H.J. Wan, Y. Yang, H.W. Xiang, Y.W. Li, "Study on the iron-silica interaction of a co-precipitated Fe/SiO_2 Fischer-Tropsch synthesis catalyst", Catal. Comm., vol. 7, pp. 733-738, Apr. 2006.
[15] F. del Monte, M.P. Morales, D. Levy, A. Fernandez, M. Ocana, A. Roig, E. Molins, K. O'Grady, "Formation of γ-Fe_2O_3 isolated nanoparticles in a silica matrix", C.J. Serna. Langmuir, vol. 13, pp. 3627-3634, July 1997.
[16] T. Matsuzaki, K. Takeuchi, T.Hanaoka, H. Arakawa, Y. Sugi, "Hydrogenation of carbon monoxide over highly dispersed cobalt catalysts derived from cabalt(II) acetate", Catalysis Today, vol. 28, pp. 251-259, May 1996.
[17] L.M. Tau, R. Robinson, R. D. Ross, B.H. Davis, "Oxygenates formed from ethanol during Fischer-Tropsch synthesis", J. Catal., vol. 105, pp. 335-341, June 1987.
[18] X.D. Xu, E.B.M. Doesburg, J.J.F. Scholten, "Synthesis of higher alcohols from syngas – recently patented catalysts and tentative ideas on the mechanism", Catalysis Today, vol. 2, pp. 125-170, Dec. 1987.
[19] Y. Liu, B.T. Teng, X.H. Guo, Y. Li, J. Chang, L. Tian, et al., "Effect of reaction conditions on the catalytic performance of Fe-Mn catalyst for

Fischer-Tropsch synthesis", J. Mol. Catal. A: Chemical, vol. 272, pp. 182-190, July. 2007.
[20] H. Schulz, H. Gokcebay, "Catalysis of organic reactions", vol. 18, J.R. Kosak, Ed. New York: Marcel Dekker, 1984, pp.153-169.
[21] M.E. Dry, "Catalysis-science and technology", vol. 1, Anderson and Boudart, Ed. New York: Springer Verlag, 1981, p. 159.
[22] A. Kiennemann, A. Barama, S. Boujana, M.M. Bettahar, "Higher alcohol synthesis on modified iron based catalysts: Copper and molybdenum addition", Appl. Catal. A, vol. 99, pp. 175-194, June. 1993.